American Journal of Condensed Matter Physics 2013, 3(3): 80-88
DOI: 10.5923/j.ajcmp.20130303.03

Spectroscopic Properties of Pr^{3+} in Lithium Bismuth Borate Glasses

Beena Bhatia[1], Vishal parihar[1], Sanjay Singh[2], A. S. Verma[3,*]

[1]Ceramics Laboratories, Department of Physics, Jai Narain Vyas University Jodhpur, 342001, India
[2]Department of Physics, Shyam Lal College, University of Delhi, Delhi, 110032, India
[3]Department of Physics, Banasthali Vidyapith, Rajasthan, 304022, India

Abstract Glasses of the system: xB_2O_3-$10Bi_2O_3$-$30Li_2O$-xPr_6O_{11} where x =1, 1.5 and 2 were prepared by melt quenching technique. Optical absorption and emission spectra have been recorded. The intensities of f-f transitions are calculated in term of Judd-Ofelt (JO) intensity parameters Ω_λ (λ = 2, 4 and 6). Using the fluorescence data and these Ω_λ parameters, various radiative properties like transition probability (A), branching ratio (β_R), radiative lifetime (τ_R), and stimulated emission cross section (σ_p), of various emission lines have been evaluated. The values of these parameters indicate that for blue ($^3P_0 \rightarrow {}^3H_4$, 491 nm) transition can be considered to be good laser transition in the visible region.

Keywords Doped Lithium Bismuth Borate Glasses, Judd-Ofelt Analysis, Optical Properties, Rare Earth Elements

1. Introduction

Rare earth ion doped glasses are often used as lasing materials for glass lasers, light emitting diode, memory device and fiber amplifiers for optical telecommunication. Among the lanthanides ions trivalent Praseodymium (Pr^{3+}) has wide applications such as up-converters [1], fiber amplifiers in 1.3 μm region[2], UV, visible and near infrared lasers[3], electro optic device[4-6] and optical fiber laser[7] due to a large number of available absorption bands in UV-VIS-NIR region. There has been increasing interest in synthesis, structure and physical properties of heavy metal oxide (HMO) glasses such as Bi_2O_3, PbO, GeO_2, GaO_2 etc.[8-11]. It has been reported that lithium bismuth borate glasses containing Bi_2O_3 as the network intermediate(NWI) to the glass network former B_2O_3 (NWF) possess high refractive index, high infrared transparency , high density, moisture resistant and have extended transmission in mid IR region. The addition of network modifier (NWM) Li_2O is to improve both electrical and mechanical properties of such glasses.

* Corresponding author:
ajay_phy@rediffmail.com (A. S. Verma)
Published online at http://journal.sapub.org/ajcmp

In the present work, we have studied on the absorption and emission properties of Pr^{3+} doped lithium bismuth borate glasses. The Judd-Ofelt[12, 13] theory has been applied to compute the intensity parameters Ω_λ (λ = 2, 4 and 6). These intensity parameter have been used to evaluate important optical properties such as radiative transition probability for spontaneous emission, branching ratio, radiative life time of the excited state and stimulated emission cross section in order to optimize the best configuration of the rare earth ions- host to improve the laser efficiency of a given electronic transition. To understand the laser efficiency of these materials, the value of spectroscopy quality factor (Ω_4/ Ω_6) has been evaluated.

2. Experimental

2.1. Glass Preparation

The following molar compositions with rare earth doped and reference glass samples were prepared by melt quenching technique.

Glass- R $60B_2O_3$-$10Bi_2O_3$-$30Li_2O$
Glass- A $59B_2O_3$-$10Bi_2O_3$-$30Li_2O$-$1Pr_6O_{11}$
Glass- B $58.5B_2O_3$-$10Bi_2O_3$-$30Li_2O$-$1.5Pr_6O_{11}$
Glass- C $58B_2O_3$-$10Bi_2O_3$-$30Li_2O$-$2.0Pr_6O_{11}$

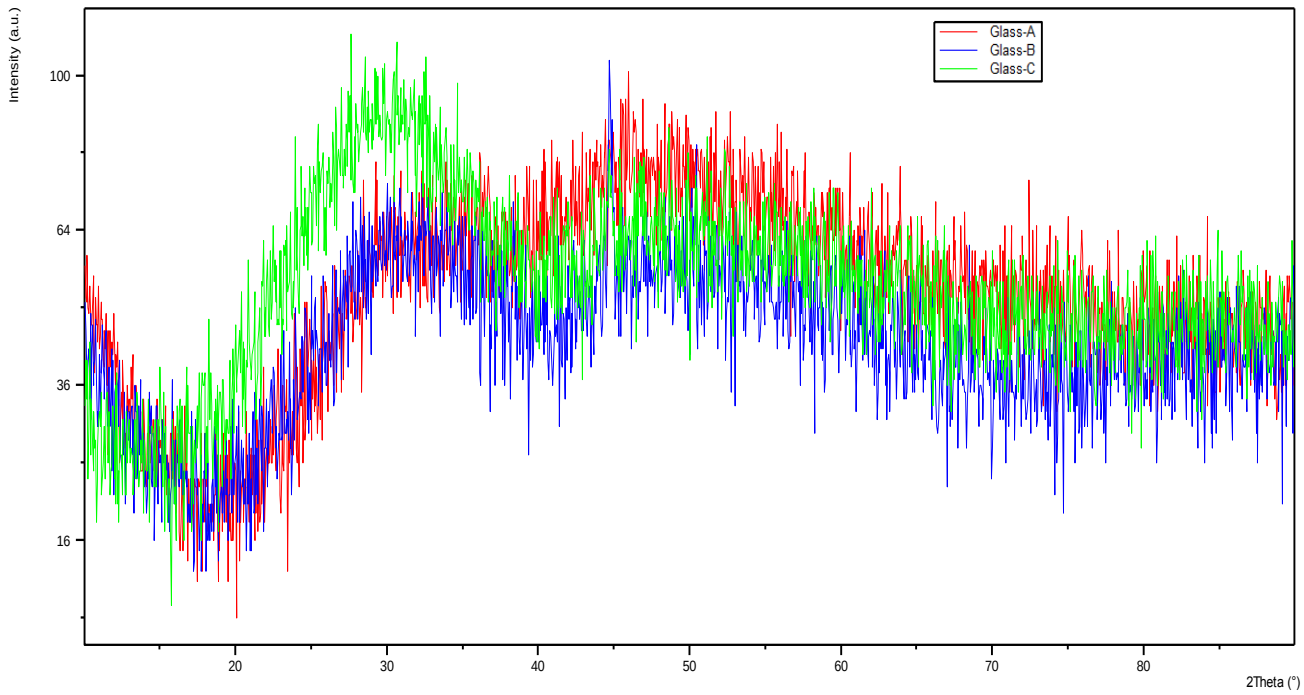

Figure 1. XRD Pattern of Pr^{3+} : LBiB glasses

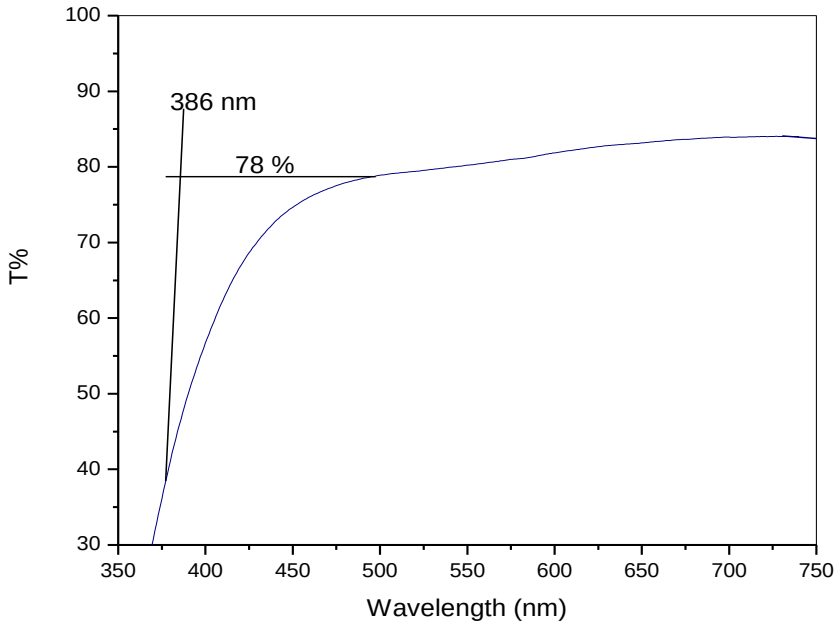

Figure 2. UV-Vis transmission spectra of LBiB glass

The starting materials used in the present work were of AR grade chemicals (H_3BO_3, Bi_2O_3, Li_2CO_3 and Pr_6O_{11}) having purity 99.99%. All weighed chemicals were powdered by using an Agate pestle mortar and mixed thoroughly. The raw mixed materials (15 g) were melted in alumina crucibles in silicon carbide based electrical furnace for 2h at 1050℃. The glass formed by quenching the melt on a pre-heated stainless steel mould was immediately transferred to muffle furnace and were annealed at temperature of 300℃ for 60 minutes to remove thermal strains and stresses. Sample of the size 20mm×15mm×1.5mm were cut and polished on all sides to make their faces flat and parallel. Every time fine powder of cerium oxide was used for polishing the samples.

The characterization of the specimens was done to ensure the glass formation by X-ray diffraction. It was recorded on PANalytical X′pert Pro MPD diffractometer of CuKα radiation (1.5406 Å) operated at 45 kV and 40 mA with a scanned step size of 0.05° and time for each step 1 sec. in the region of $2\theta = 10°$ to 90°. The absorption spectra of these glasses were recorded between wavelength ranges 400-650 and 900-2250 nm with a Perkin-Elmer Lambda 750 UV/VIS / NIR Spectrophotometer at room temperature. The emission spectra of the glass samples were recorded using Varian Make Cary Eclipse fluorescence spectrophotometer in the

spectral range 460-650 nm using the exciting wavelength 445 nm.

2.2. Physical Properties

By Appling Archimede's principle, the glass densities were measured with Xylene as an immersion liquid on a single-pan electrical balance to the nearest 0.0001 g. The error in density measurement is estimated to be ±0.004 g cm^{-3}. The refractive indices of these glasses have been measured at λ = 589.3 nm on an Abbe refractometer with an accuracy of ±0.001. The sample being glassy, it requires an adhesive coating on its surface, preferably 1-monobromonaphthalene as the contact layer between the sample and prism of the refractometer by using a sodium vapor lamp.

The rare earth ions concentration was calculated [14]

$$\text{N (ions/cm}^3) = \frac{\text{(Avogadro's number) (glass density)}}{\text{(Average molecular weight)}} \quad (1.1)$$

(mol% of rere earth)

The dielectric constant (ε) was calculated from the refractive index of the glass using[15].

$$\varepsilon = n_d^2 \quad (1.2)$$

The optical dielectric constant (pdt/dp) was calculated from the measured refractive index at 589.3 nm using the formula[16].

$$p\frac{\partial t}{\partial p} = (\varepsilon - 1) = (n_d^2 - 1) \quad (1.3)$$

Where, ε is the dielectric constant.

From the average molecular weight of the glass, the density and the total number of ions the mean atomic volume (in g/cm^3/atom) can be obtained.

The reflection loss from the glass surface was computed from the refractive index by using the Fresnel formula as shown below[17].

$$R = \left[\frac{(n_d - 1)}{(n_d + 1)}\right]^2 \quad (1.4)$$

The molar refractivity R_M for each glass was evaluated using[18]

$$R_m = \left[\frac{(n_d^2 - 1)}{(n_d^2 + 2)}\right]\frac{\overline{M}}{D} \quad (1.5)$$

Where, M is the average molecular weight and D is the density in g cm^{-3}.

The polaron radius and inter-ionic separation were calculated using the formulae[19].

$$r_p = \frac{1}{2\left(\frac{\pi}{6N}\right)^{1/3}} \quad (1.6)$$

and,

$$r_i = \left(\frac{1}{N}\right)^{1/3} \quad (1.7)$$

The electronic polarizability α_e was calculated using the formula[20]

$$\alpha_e = \frac{3(n_d^2 - 1)}{4\pi N(n_d^2 + 2)} \quad (1.8)$$

Where, N is the rare earth ions concentration.

The various physical properties calculated are reported in Table 1.

Table 1. Various physical properties of Pr^{3+} doped LBiB glasses

Physical properties	Glass- A	Glass-B	Glass- C
Refractive Index n_d, at 589.3 nm	1.656	1.657	1.658
Density, d (g/cm^3)	2.7589	2.7601	2.7632
Thickness, t (cm)	0.291	0.294	0.295
Average molecular weight $\overline{M}$ (g)	106.85	111.61	116.37
Rare earth ions concentration N ($\times 10^{21}$ ions/cm^3)	1.555	2.234	2.860
Dielectric Constant (ε)	2.742	2.746	2.749
Optical Dielectric Constant (pdt/dp)	1.742	1.746	1.749
Molar Volume V_m (gm/cm^3)	38.729	40.437	42.114
Mean atomic volume (gm/cm^3/atom)	0.0857	0.0883	0.0908
Reflection losses (R)	6.100	6.114	6.128
Molar refractivity (R_m)	14.229	14.874	15.510
Polaron radius (r_p)(A^0)	3.478	3.083	2.839
Interionic distance (r_i)(A^0)	8.632	7.650	7.045
Electronic polarizability α_e (10^{-23} ions cm^{-3})	5.642	3.932	3.075
Field strength F($10^{16} \times cm^{-2}$)	0.2406	0.3093	0.3660

3. Theoretical

3.1. Nephelauxetic Ratio (β) and Bonding Parameter ($b^{1/2}$)

The nature of the R-O bond is known by the Nephelauxetic Ratio (β) and Bonding Parameters (δ), which are computed by using following formulae[21]. The Nephelauxetic Ratio is given by

$$\beta = \frac{\nu_g}{\nu_a} \quad (1.9)$$

Where, ν_a and ν_g refer to the energies of the corresponding transition in the glass and free ion, respectively. The values of bonding parameter δ is given by

$$\delta = \frac{1 - \overline{\beta}}{\overline{\beta}} \quad (2.0)$$

Where $\overline{\beta}$ is the average value of β.

3.2. The Oscillator Strengths

The intensity of spectral lines are expressed in terms of oscillator strengths using the relation [22].

$$f_{\exp} = 4.32 \times 10^{-9} \int \varepsilon(\nu) d\nu \quad (2.1)$$

Where, ε (ν) is molar absorption coefficient at a given energy ν (cm^{-1}), to be evaluated from Beer–Lambert law.

Under Gaussian Approximation, using Beer–Lambert law, the observed oscillator strengths of the absorption bands have been experimentally calculated[23], using the modified relation:

$$f_{exp} = 4.6\times10^{-9}\times\frac{1}{cl}\log(\frac{I_0}{I})\times\Delta\nu_{1/2} \quad (2.2)$$

Where c represents the concentration of rare earth ion in the glass and 'l' is its optical path length. $\log(\frac{I_0}{I})$ is called optical density, $\Delta\nu_{1/2}$ is the half band width. In the present work, the intensities of all the bands are measured by the area method. The experimental and calculated oscillator strengths for Pr^{3+} ions in lithium bismuth borate glasses are given in Table 2.

3.3. Judd-Ofelt Parameters

According to Judd[12] and Ofelt[13] theory, independently derived expression for the oscillator strength of the induced forced electric dipole transitions between an initial J manifold $|4f^N(S, L)J>$ level and the terminal J' manifold $|4f^N(S'L')J'>$ is given by:

$$f_{JJ'} = \frac{8\pi^2 mc\nu}{3h(2J+1)}\left[\frac{(n^2+2)^2}{9n}\right]\times S(J, J') \quad (2.3)$$

Where, the line strength S (J, J') is given by the equation

$$S(J, J') = e^2 \sum_{\lambda=2,4,6} \Omega_\lambda \langle 4f^N(S, L) J \| U^{(\lambda)} \| 4f^N(S', L')J' \rangle^2 \quad (2.4)$$

In the above equation m is the mass of an electron, c is the velocity of light, ν is the wave number of the transition, h is Planck's constant, n is the refractive index, J and J' are the total angular momenta of the initial and final level respectively, Ω_λ (λ = 2, 4 and 6) are known as Judd-Ofelt intensity parameters which contain the effect of the odd-symmetry crystal field terms, radial integrals and energy denominators. $\|U^{(\lambda)}\|^2$ are the matrix elements of the doubly reduced unit tensor operator calculated in intermediate coupling approximation. Ω_λ parameter can be obtained from least square fitting method[24] (Table 3). The matrix element $\|U^{(\lambda)}\|^2$ that are insensitive to the environment of rare earth ions ware taken from the literature[25].

Table 2. Measured ($f_{exp}\times10^{+6}$) and calculated ($f_{exp}\times10^{+6}$) oscillator strength of Pr^{3+} ions in lithium bismuth borate glasses

Energy level from $^3H_4\rightarrow$	Glass-A		Glass-B		Glass-C	
	f_{exp}	f_{cal}	f_{exp}	f_{cal}	f_{exp}	f_{cal}
$^3P_2$	7.485	2.542	6.513	2.140	5.820	1.632
$^3P_1$	3.466	2.500	2.176	1.564	1.696	1.162
$^3P_0$	2.539	2.479	1.715	1.551	1.687	1.152
$^1D_2$	1.721	7.592	1.241	0.644	1.162	4.921
$^1G_4$	0.163	0.220	0.154	0.188	0.124	1.429
$^3F_4$	2.252	2.422	1.977	2.143	1.563	1.643
$^3F_3$	5.068	4.565	4.180	3.768	3.276	2.868
$^3F_2$	2.267	1.992	2.112	1.888	1.684	1.441
r.m.s. deviation	±1.825		±1.586		±1.533	

Table 3. Judd-Ofelt intensity parameters (Ω_2, Ω_4, Ω_6) of Pr^{3+} doped glasses

Glass	Ω_2 (10^{-20} cm^2)	Ω_4 (10^{-20} cm^2)	Ω_6 (10^{-20} cm^2)	Ω_4 / Ω_6	Reference
LBiBA	0.314	3.788	3.555	1.07	Present work
LBiBB	1.299	2.368	3.210	0.74	Present work
LBiBC	1.023	1.759	2.460	0.72	Present work
Oxyfluoride	0.13	4.09	6.33	0.65	[28]
L4BP	0.13	4.61	3.92	1.18	[25]
L5BP	0.98	5.85	5.36	1.09	[25]
PBOF	0.02	7.88	4.81	1.64	[29]
ZBLA	0.24	4.50	5.40	0.83	[30]
YSZ	0.34	7.25	3.25	2.23	[31]
LiTfP	0.264	8.067	5.884	1.37	[4]
NaTfP	0.229	7.312	6.149	1.19	[4]
KTFP	0.498	8.814	6.426	1.37	[4]
ZnCdF	0.72	4.80	7.93	0.61	[32]
InF2	0.80	4.33	7.26	0.60	[33]

3.4. Radiative Properties

The Ω_λ parameters obtained using the absorption spectral results have been used to predict radiative properties such as spontaneous emission probability (A) and radiative life time (τ_R), and laser parameters like fluorescence branching ratio (β_R) and stimulated emission cross section (σ_p).

The spontaneous emission probability from initial manifold $|4f^N (S', L') J'>$ to a final manifold $|4f^N (\bar{S}, \bar{L}) \bar{J}>|$ is given by:

$$A[(S', L') J'; (\bar{S}, \bar{L}) \bar{J}] = \frac{64\pi^2 \nu^3}{3h(2J'+1)} \left[\frac{n(n^2+2)^2}{9}\right] \times S(J', \bar{J}) \quad (2.5)$$

Where, $S(J', \bar{J}) = e^2[\Omega_2 \left\|U^{(2)}\right\|^2 + \Omega_4 \left\|U^{(4)}\right\|^2 + \Omega_6 \left\|U^{(6)}\right\|^2]$

For Pr^{3+} ion, $J' = 0$ or 1 and matrix elements of the doubly reduced unit tensor operator reported by P. Babu et al.[25] have been used.

The fluorescence branching ratio for the transitions originating from a specific initial manifold $|4f^N(S', L')J'>$ to a final manifold $|4f^N (\bar{S}, \bar{L}) \bar{J}>$ is given by

$$\beta[(S', L') J'; (\bar{S}, \bar{L}) \bar{J}] = \frac{A[(S', L') J'; (\bar{S}, \bar{L}), \bar{J}]}{\sum_{\bar{S},\bar{L},\bar{J}} A[(S', L') J'; (\bar{S}, \bar{L}), \bar{J}]} \quad (2.6)$$

Where, the sum is over all terminal manifolds. In the case of Pr^{3+} ion, the terminal manifold are $^3P_2$, $^1I_6$, $^3P_{1,0}$, $^1D_2$, $^1G_4$, $^3F_{4,3,2}$ and $^3H_{6,5,4}$.

The radiative life time is given by

$$\tau_{rad} = \sum_{\bar{S},\bar{L},\bar{J}} A[(S', L') J'; (\bar{S}, \bar{L}) \bar{J}]^{-1} = A_{Total}^{-1} \quad (2.7)$$

Where, the sum is over all possible terminal manifolds.

The stimulated emission cross-section for a transition from an initial manifold $|4f^N (S', L') J'>$ to a final manifold $|4f^N (\bar{S}, \bar{L}) \bar{J}>|$ is expressed as

$$\sigma_p(\lambda_p) = \left[\frac{\lambda_p^4}{8\pi c n^2 \Delta\lambda_{eff}}\right] \times A[(S', L') J'; (\bar{S}, \bar{L}) \bar{J}] \quad (2.8)$$

Where, λ_p the peak fluorescence wavelength of the emission band and $\Delta\lambda_{eff}$ is the effective fluorescence line width.

Table 4. Emission peak wavelengths ($\lambda_{p,}$), radiative transition probability (A_{rad}), branching ratio (β), stimulated emission cross-section ($\sigma_p(\Delta\lambda_{eff})$), total radiative transition probability (A_T), radiative life time (τ_r) and total emission cross-section($\sigma_t(\Delta\lambda_{eff})$) for various transitions in Pr^{3+} doped LBiB glasses

Transition		LBiB-A			LBiB-B			LBiB-C		
	λ_{max} (nm)	$A_{rad}(s^{-1})$	β	σ_p (10^{-20} cm^2)	$A_{rad}(s^{-1})$	β	σ_p (10^{-20} cm^2)	$A_{rad}(s^{-1})$	β	σ_p (10^{-20} cm^2)
$^3P_0 \rightarrow {}^3H_4$	491	16411	0.6232	3.86	10279	0.5173	2.64	7706	0.4649	1.54
$^3P_1 \rightarrow {}^3H_5$	530	9349	0.3848	3.58	6463	0.3019	2.74	4852	0.2450	1.85
$^3P_0 \rightarrow {}^3H_5$	542	-	-	-	-	-	-	-	-	-
$^3P_1 \rightarrow {}^3H_6$	567	-	0.0945	-	-	0.1073	-	-	0.1160	-
$^3P_0 \rightarrow {}^3H_6$	606	3469	0.1317	2.26	3139	0.1580	1.86	2415	0.1457	1.31
		$A_T(^3P_0) = 26333\ s^{-1}$, $\tau_{rad}(^3P_0) = 38\ \mu s$ $A_T(^3P_1) = 24297\ s^{-1}$, $\tau_{rad}(^3P_1) = 41\ \mu s$			$A_T(^3P_0) = 19871\ s^{-1}$, $\tau_{rad}(^3P_0) = 50\ \mu s$ $A_T(^3P_1) = 21411\ s^{-1}$, $\tau_{rad}(^3P_1) = 47\ \mu s$			$A_T(^3P_0) = 16574\ s^{-1}$, $\tau_{rad}(^3P_0) = 60\ \mu s$ $A_T(^3P_1) = 19800\ s^{-1}$, $\tau_{rad}(^3P_1) = 50\ \mu s$		

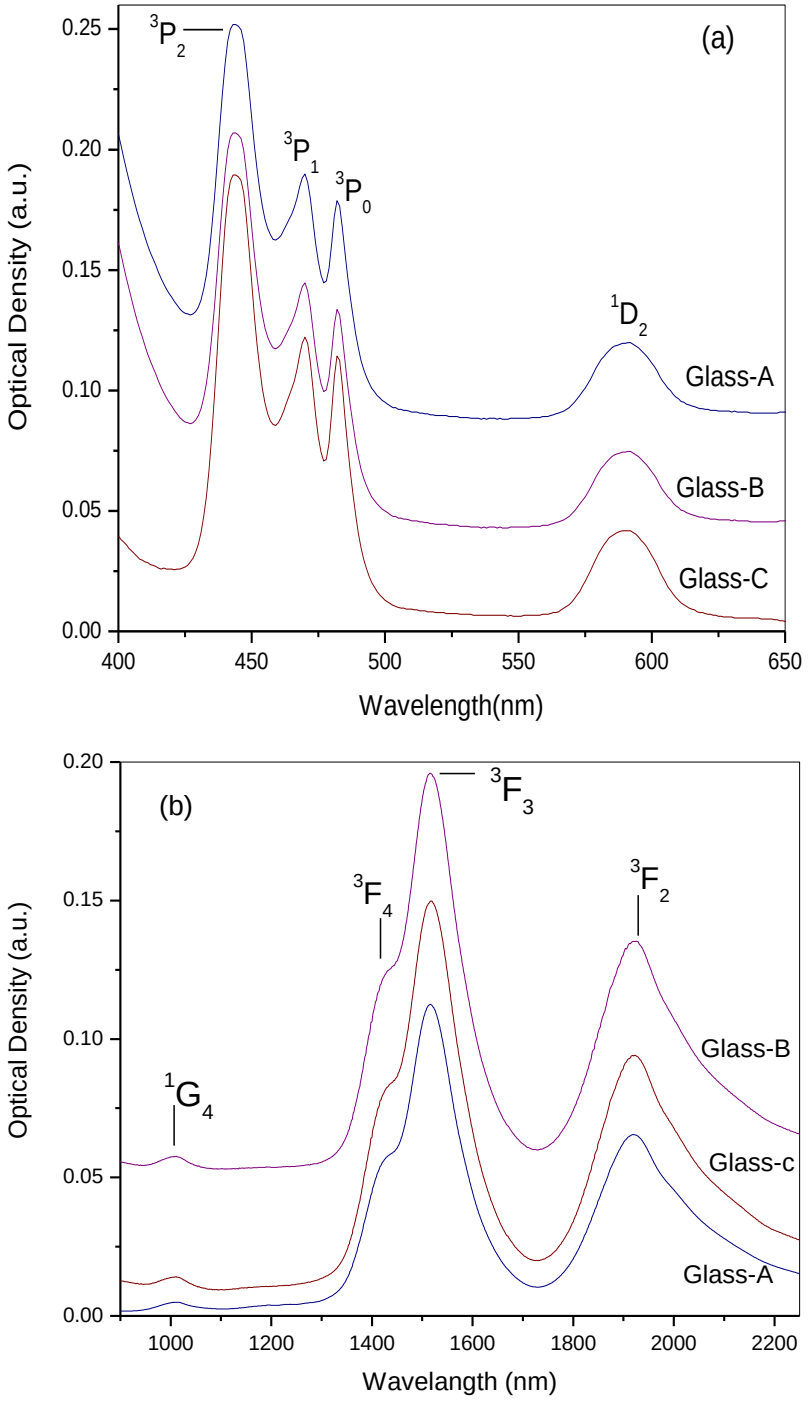

Figure 3. Optical absorption spectra of Pr^{3+}: LBiB glasses (a) UV-Vis region (b) NIR region

4. Results and Discussion

The amorphous nature of all samples was confirmed by the absence of Bragg's peak in X-ray diffraction pattern (Fig. 1). The various physical properties of all the glass samples are presented in Table 1. The electronic polarizability ($\alpha_{e)}$, polaron radius (r_p), inter ionic distance (r_i) slightly decrease with the increase of rare earth ion concentration. The value of nephelauxetic ratio and bonding parameters may be positive or negative indicating covalent or ionic bonding. It is found that all Pr^{3+} glasses under study have covalent bonding nature. The optical absorption spectra of Pr^{3+} doped xB_2O_3-$10Bi_2O_3$-$30Li_2O$-xPr_6O_{11} (where x =1,1.5 and 2 mol%) glass samples are measured at room temperature in the wavelength ranges 400-650 and 900-2250 nm and are shown in Fig. 3. The optical absorption bands around the $^3P_2$ (443nm), $^3P_1$ (469 nm), $^3P_0$ (482 nm), $^1D_2$ (591 nm), $^1G_4$ (1008 nm), $^3F_4$ (1441 nm), $^3F_3$ (1519 nm) and $^3F_2$ (1922 nm),

are assigned from the ground state, $^3H_4$. Assignments have been made by published article [26]. The observed absorption bands can be divided into three groups, transition from $^3H_4 \rightarrow {}^1G_4$ and $^3H_4 \rightarrow {}^3F_{4,3,2}$ in the infrared region, the $^3H_4 \rightarrow {}^1D_2$ transition at 591 nm and $^3H_4 \rightarrow {}^3P_{2,1,0}$ complex group of transitions in violet to blue region. From the absorption spectra, experimental oscillator strengths have been calculated for all the absorption bands. Further, Judd–Ofelt intensity parameters Ω_λ (λ = 2, 4, and 6) were calculated by using the fitting approximation of the experimental oscillator strengths to the calculated oscillator strengths with respect to their electric dipole contributions. The fairness of the fitting approximation is examined by the root mean square deviations (δ_{rms}). Low δ_{rms} values clearly indicate the accuracy of fitting. The experimental, calculated oscillator strengths and Judd–Ofelt intensity parameters of all Pr^{3+} lithium bismuth borate glasses are presented and compared with the other glass systems which are listed out in Table 2. From Table 2, it is observed that, for the transition $^3H_4 \rightarrow {}^3P_2$ at 443 nm, the oscillator strength is very high compared with the other absorption transitions in all glasses. Thus, the transition $^3H_4 \rightarrow {}^3P_2$ is known as the hypersensitive transition and follows the selection rules $\Delta S = 0$, $\Delta L = 2$, and $\Delta J \leq 2$ [27]. Table 3 shows that Ω_2 increases whereas Ω_4 and Ω_6 decrease with increase in the Pr_6O_{11} content in host glasses. The order of magnitude of Judd-Ofelt intensity parameter is $\Omega_4 < \Omega_6 < \Omega_2$ for glass-A and $\Omega_6 < \Omega_4 < \Omega_2$ for glass-B and glass-C. These intensity parameters reflect the local structure and bonding in the vicinity of rare earth ions to some extent. As a general conclusion, Ω_2 parameter increases with asymmetry of the local structure and with the degree of covalency of the lanthanide-ligand bonds, wherease Ω_6 parameter decreases with the tendency of covalency. Ω_2 is higer for the present glasses in comparison to oxy-fluoride[28], lithium borate[25], PBOF[29], ZBLA[30], yttria-stabilized-zirconia (YSZ: ZrO_2 -Y_2O_3)[31], tellufluoro-phosphate[4], ZnCdF (ZnF_2 –CdF_2)[32] and InF2[33]. Weber and Jacob[34] have reported that the ratio (Ω_4/Ω_6) known as the spectroscopic quality factor characterizes the glass concerned. The values of (Ω_4/Ω_6) for glasses under study are given in Table 3. Glass-A is having larger value of (Ω_4/Ω_6) than other two glasses and it shows that glass-A is a kind of better optical glass.

Fig. 2 shows the transmission spectra of reference glass (LBiB glass) in the UV-Vis range. It is clear from this figure that, the LBiB glass has above 78% transmission in the optical window up to 0.387 µm. Fig. 4 present the excitation spectrum of Pr^{3+} ions doped glasses, which was measured by monitoring an intense emission at 606 nm. The excitation peaks from the excitation spectrum are assigned electronic transition with ground level $^3H_4$ to higher energy level of Pr^{3+}, i.e., $^3H_4 \rightarrow {}^3P_0$ (491.5 nm). Fig 5 shows the emission spectra of Pr^{3+}: LBiB glasses, the most intense band in the absorption spectra around $^3P_2$ level with 445 nm (diode laser) has been used for the excitation of Pr^{3+} ions. As a consequence of which, three strong fluorescence bands around 491, 530 and 606 nm, have been observed in the wavelength region 450-650 nm. The very weak fluorescence bands around 542 and 567 nm are not included in the analysis because of the uncertainties in the $\Delta\lambda_{eff}$ determination.

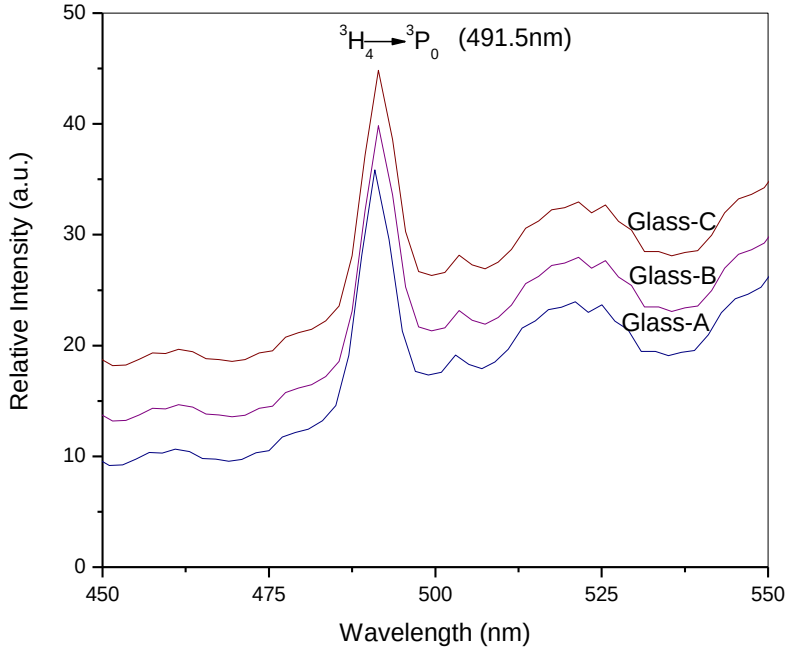

Figure 4. Excitation spectrum of Pr^{3+}: LBiB glasses

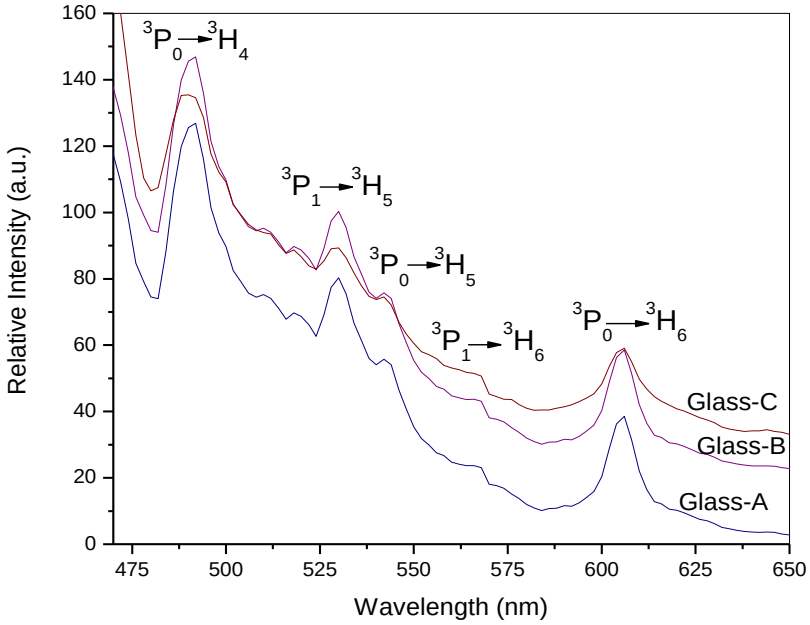

Figure 5. Emission spectrum of Pr^{3+}: LBiB glasses

The fluorescence peaks are assigned $^3P_0 \rightarrow {}^3H_{4,5,6}$ and $^3P_1 \rightarrow {}^3H_{5,6}$ transition, respectively. The assignment of the peaks to specific transitions have been made on the basis of known energy level of Pr^{3+} ions as reported by Dieke[35] and earlier workers[25,26]

Among these, the transition $^3P_0 \rightarrow {}^3H_4$ at 491 nm is a lasing transition having prominent intensity. From the emission spectra, it is also observed that the fluorescence quenching occurs with the increase of concentration beyond certain limit. Emission intensity of Pr^{3+}: LBiB glasses increases with the increase of Pr^{3+} concentration from 1 and 1.5 mol% and reaches the maximum value at x = 1.5 mol% and then decreases indicating the concentration quenching phenomena. For Pr^{3+} concentrations more than 1.5 mol%, the emission intensity was quenched because at higher concentrations the interactions between Pr^{3+} ions increases and causes the energy transfer process[36]. By using the Judd–Ofelt intensity Ω_λ (λ = 2, 4, and 6) parameters, radiative properties of emission transitions of Pr^{3+}: LBiB glasses have been computed and the results relating to spontaneous emission probability (A), radiative life time (τ_R), fluorescence branching ratio (β_R) and stimulated emission cross section (σ_p) of the various emission transitions are calculated and are presented in Table 4. The value of spontaneous emission probability (A) for Pr^{3+}: LBiB glasses are found to be maximum for transition $^3P_0 \rightarrow {}^3H_4$ suggesting them to be probable laser transition. From the Table 4, it is observed that the branching ratios of the transition $^3P_0 \rightarrow {}^3H_4$ for Pr^{3+}: LBiB glasses are found to be maximum compared with other transition. Normally, the magnitude of branching ratio would be higher for the lasing transitions than those for the other transitions. Table 4, indicates that the two transitions $^3P_0 \rightarrow {}^3H_4$ and $^3P_1 \rightarrow {}^3H_5$ are found suitable for laser excitation. Further, the stimulated emission cross section (σ_p) value describes the laser performance of a material and also estimates the rate of energy extracted from the lasing materials.

Pr^{3+}: LBiB glasses $^3P_0 \rightarrow {}^3H_4$ transition can be considered to be good laser transition in the visible region for blue ($^3P_0 \rightarrow {}^3H_4$, 491 nm) wavelength.

5. Conclusions

Optical absorption and fluorescence analyses of Pr^{3+} doped lithium bismuth borate glasses have been performed. The Judd–Ofelt model has been applied to calculate the JO intensity parameters Ω_λ (λ = 2, 4, and 6) from the measured oscillator strength of the absorption spectra of Pr^{3+}: LBiB glasses. From the magnitudes of the bonding parameter δ, for Pr^{3+} ions in various glasses, it is found that Pr^{3+} ions have a covalent character in all the glasses. The spectroscopic quality factor (Ω_4/Ω_6), branching ratio (β_R) and the stimulated emission cross section (σ_p) values are calculated for present glasses. It could be observed that glass-A possess better values compared to the other two glass (B and C) system. The large stimulated emission cross section in lithium bismuth borate glasses suggests the possibility of utilizing these systems as laser materials. Thus, we could suggest that Pr^{3+}: LBiB glasses are the suitable potential candidates for laser materials for blue ($^3P_0 \rightarrow {}^3H_4$, 491 nm) wavelength.

ACKNOWLEDGEMENTS

The authors are thankful to Prof. S.S.L. Surana, Jai Narain Vyas University, Jodhpur (Raj.) for his help in optical absorption measurements.

REFERENCES

[1] D.B. Gatch, S.A. Holmstrom, and W.M. Yen, J. Lumin. 83-84 (1999) 55.

[2] Y. Zhao, S. Fleming, IEEE J. Quant. Electron. 33 (1997) 905.

[3] A.A. Kaminskii, Laser Crystals, 2nd Edition, Springer, Berlin 1990.

[4] R. Moorty, M. Jagasin, Mater. Chem. Phys. 93 (2005) 455.

[5] Y.K. Sharma, S.P. Tandon, S.S. Surana, Mater. Sci. Eng. B 77 (2000) 167.

[6] Y.C. Ratnakaram, A.V. Kumar, D.T. Naidu, N.O. Gopal, Mater.Lett. 58 (2004) 3908.

[7] D.M. Baney, L. Yang, J.Ratcliff, K.W. Chang, Electron. Lett. 31 (1995) 1842.

[8] C.H. Kam and S. Buddudu, J. Quant. Spectrosc. Radiant. Trans 325-337 (2004) 87.

[9] G.A. Kumar, A. Martinez, E. Mejia and C.G. Eden, J. Alloys. Comp. 117-120 (2004) 365.

[10] E. Culea, L. Pop and S. Simoon, Mater. Sci. Engg. 59-63 (2004) B 112.

[11] J. Yang, S. Dai, Y. Zhou, Leiwen. Lili Hu and Z.H. Jiang, Appl. Phys. 977-983 (2003) 93 (2).

[12] B.R. Judd, Phys. Rev. 127 (1962) 750.

[13] G.S. Ofelt, J. Chem. Phys. 37 (1962) 511.

[14] A. Shankar, A. Dasgupta, B. Babsu, A. Paul, J. Mater. Sci. Lett. 4 (1983) 697.

[15] B. Bendow, P. K. Banerjee, M.G. Drexhage and J. Lucas, J. Am. Ceram. Soc. 65 (1985) C 92.

[16] J. Schroeder, J. Non-Cryst. Solids 40 (1980) 549.

[17] Y. Ohisti, S.Mitachi and T. Tanabe, Phys. Chem. Glasses 24 (1983) 135.

[18] J.E. Shelby, and J. Ruller, Phys. Chem. Glasses 28 (1987) 262.

[19] M.M. Ahmed, C.A. Hogarth and M.N. Khan, J. Mater. Sci. Lett. 19 (1984) 4040.

[20] A. Klonkowski, J. Non-Cryst. Solids 72 (1985) 117.

[21] S.P. Sinha, in: Complexes of the rare earths. Oxford: Pergamon Press; 1996.

[22] C. Gorller-Walrand, K. Binnemans, Spectral intensities of f-f transition, in: K.A. Gschneidner Jr., L. Eyring (Eds.), Handbook on the physics and Chemistry of rare earths, Vol. 25, North-Holland. Amsterdom, 1998 (Chapter 167).

[23] Y.K. Sharma, S.S.L. Surana and R. K. Singh, J. of Rare Earth. 773 (2009) 27 (5).

[24] C.H. Goublen, Mathods of Statistical Analysis, Asian Publishing House, Bombay, Ch. 8 (1964) 138.

[25] P. Babu and C.K. Jayasankar, Physica B 326-340 (2001) 301.

[26] I. Pal, A. Agarwal, S. Sanghi, M.P. Aggarwal, J. Alloys comp. 7625-7631 (2011) 509.

[27] S. Tanabe, T. Ohyagi, N. Soga, T. Hanada, Phys. Rev. B 46 (1992) 3305.Za

[28] R.T. Genova, I.R. Martine, U.R.R. Mendoza, F. Lahoz, A.D.L. Garrin, P. Nunez, J.G. Platas, V. Lavine, J. Alloys Compd. 380 (2004) 167.

[29] P. Nachimuthu, R. Jagannathan, Phys. Chem. Glasses 36 (1995) 77.

[30] M. Eyal, E. Greenberg, R. Reisfeld, Chem. Phys. Lett. 117 (1985) 108.

[31] B. Savoini, J.E. Munoz Santiuste, R. Gonzalez, Phys. Rev. B 56 (1997) 5856.

[32] M.A. Bunuel, R. Cases, M.A. Chamarro, R. Alcala, Phys. Chem. Glasses 33 (1992) 16.

[33] A.B. Arauzo, R. Cases, R. Alcala, Phys. Chem. Glasses 35 (1994) 202.

[34] R.R. Jacobs, M J. Weber, IEEE J. Quant. Electron. 12 (1976) 102.

[35] G.H. Dieke, Spectral and Energy Level of Rare Earth Ions in Crystal, Interscience, New York, 1968.

[36] Q. Nie, X. Li, S. Dai, T. Xu, Z. Jin,X. Zhang, Spectrochim Acta A 70 (2008) 537.